JOURNAL OF GEOPHYSICAL RESEARCH, VOL. 108, NO. A10, 8037, doi:10.1029/2003JA009914, 2003

# Anomalous cosmic ray intensity variations in the inner and outer heliosphere during the solar cycle 22 recovery phase (1991–1999)

M. E. Hill and D. C. Hamilton
Department of Physics, University of Maryland, College Park, Maryland, USA

J. E. Mazur
Space Sciences Department, The Aerospace Corporation, El Segundo, California, USA

S. M. Krimigis
Applied Physics Laboratory, The Johns Hopkins University, Laurel, Maryland, USA

Received 27 February 2003; revised 21 May 2003; accepted 27 May 2003; published 29 October 2003.

[1] Differential intensity measurements of interplanetary H, He, and O ions made with the Low-Energy Charged Particle (LECP) instruments aboard the Voyager 1 (V1) and Voyager 2 (V2) deep space probes and the Low-Energy Ion Composition Analyzer (LICA) aboard the near-Earth Solar Anomalous Magnetospheric Particle Explorer (SAMPEX) satellite provide a comprehensive perspective on the transport of anomalous cosmic ray (ACR) ions during the 1991–1999 recovery phase of solar cycle 22 in both the outer and inner heliosphere. We report fifteen unique, independent ACR intensity time series, ranging over kinetic energies from 0.6 to 40 MeV/nucleon, and parameterize these observations (supplemented by one time-intensity profile from the literature) with a four-parameter fitting function to quantify the ACR behavior as solar minimum conditions developed and the V1 and V2 probes ranged from 36 to 76 AU from the Sun. We discuss a possible physical explanation for the striking differences between the outer heliospheric ACR recovery profiles at various energies. The intensities of nearly all species and energies recovered similarly from 1991 to mid-1994, increasing about an order of magnitude, but differed in a rigidity-dependent manner during the subsequent 5 years with the low-rigidity particle intensities growing exponentially, increasing up to an order of magnitude, while the high-rigidity particle intensities remained nearly constant. We find that these observations support the interpretation that before 1994 the recovery profiles of all the ACRs were governed by a temporal mechanism probably driven by the timescale of the variation of the transport properties of the interplanetary medium itself, rather than the "relaxation" timescale for diffusive equilibrium to develop. After 1994 the motion of the Voyager probes through regions with stable, positive radial intensity gradients explains the diverse recovery profiles of the various ACR species. *INDEX TERMS:* 2104 Interplanetary Physics: Cosmic rays; 2114 Interplanetary Physics: Energetic particles, heliospheric (7514); 7859 Space Plasma Physics: Transport processes; 2162 Interplanetary Physics: Solar cycle variations (7536); 2152 Interplanetary Physics: Pickup ions; *KEYWORDS:* anomalous cosmic ray, time intensity profile, particle transport, cosmic ray recovery, Voyager, SAMPEX

**Citation:** Hill, M. E., D. C. Hamilton, J. E. Mazur, and S. M. Krimigis, Anomalous cosmic ray intensity variations in the inner and outer heliosphere during the solar cycle 22 recovery phase (1991–1999), *J. Geophys. Res.*, *108*(A10), 8037, doi:10.1029/2003JA009914, 2003.

## 1. Introduction

[2] As the solar system and heliosphere move with respect to the local interstellar cloud within which they are embedded, ambient interstellar neutral atoms penetrate a significant distance into the heliosphere before becoming ionized through either charge exchange with the solar wind plasma or interactions with solar UV photons [*Fisk et al.*, 1974]. After ionization, these "pick-up" ions interact with the interplanetary (IP) magnetic field, acquire energies of order 1-keV/nucleon, and are carried away from the Sun with the expanding supersonic solar wind flow until reaching the putative termination shock (TS) of the solar wind. At the TS some pick-up ions are thought to be accelerated to energies from roughly 1 to 100 MeV/nucleon, at which time they become so-called anomalous cosmic ray (ACR) ions [*Pesses et al.*, 1981], which have been widely observed

0148-0227/03/2003JA009914$09.00

during solar cycle 22 in the inner [e.g., *Selesnick et al.*, 2000; *Mazur et al.*, 2000] and outer heliosphere [e.g., *Stone et al.*, 1996; *McDonald et al.*, 2000b; *Hill et al.*, 2002; *Cummings et al.*, 2002]. In fact the discovery of ACRs [*Garcia-Munoz et al.*, 1973; *Hovestadt et al.*, 1973; *McDonald et al.*, 1974] predates that of pick-up ions [*Möbius et al.*, 1985; *Gloeckler et al.*, 1993], observations of the former being the impetus for the theoretical prediction [*Fisk et al.*, 1974] of the latter.

[3] The transport of ACRs in the heliosphere is believed to be well understood in terms of the cosmic ray transport equation (CRTE), which is the Fokker-Planck equation that *Parker* [1965] used to describe the convection, diffusion, and adiabatic energy loss processes undergone by energetic particles in the IP medium, as extended by the work of Jokipii [e.g., *Jokipii*, 1990] and his collaborators [e.g., *Jokipii et al.*, 1977; *Jokipii and Kopriva*, 1979; *Pesses et al.*, 1981] who incorporated the effects of particle drift into the resulting drift/diffusion theory. Despite the widespread use of the drift/diffusion theory to describe ACR and galactic cosmic ray (GCR) phenomena, the relative importance of the four transport processes (convection, diffusion, adiabatic cooling, and drift) is still not known. One method to learn more about ACR transport is to study their energy spectra, as has been done for solar cycle 22 by *McDonald et al.* [1995], *Stone et al.* [1996], and *Hill et al.* [2002]. Such spectral measurements were used by *Steenberg* [1998] to systematically model ACR transport using time-asymptotic numerical solutions to the CRTE that are dependent on rigidity, latitude, and radius. Another method to study ACR phenomena, and the one that is followed in this paper, is to analyze the intensity of an ACR species having energies of a given range, as a function of time (i.e., a time-intensity profile). A great deal of work in this vein has been performed by McDonald and his collaborators [*McDonald et al.*, 1994, 1998, 2000a, 2000b, 2002].

[4] In this paper a systematic study of the transport of ACRs is made by examining the time-intensity profiles of ACR H, He, and O during the recovery phase of solar cycle 22, from 1991 to 1999. Both the outer heliosphere, utilizing measurements from the LECP instruments [*Krimigis et al.*, 1977] on the Voyager 1 (V1) and Voyager 2 (V2) deep space probes, and the inner heliosphere, utilizing polar cap observations from the LICA instrument [*Mason et al.*, 1993] aboard SAMPEX in low-Earth orbit, are studied herein. Preliminary reports were made by *Hamilton et al.* [1997, 1999], *Hill et al.* [2001b], and *Hill* [2001] and this work is the second in a series of papers studying ACR transport phenomena during the solar cycle 22 recovery period, the first of which [*Hill et al.*, 2002] focused on the evolution of ACR energy spectra. A related paper [*Hill et al.*, 2001a] also studied the temporal variations of outer heliospheric ACR intensities but only during a restricted time period, 1998–1999, and for the express purpose of examining ~150-day periodicities, not large-scale transport; therefore that paper is not identified as being part of the present series. The present paper extends the work (regarding ACR time-intensity profiles) of other investigators to significantly lower energies, including particles with energies from 0.3 to 38 MeV/nucleon. Additional papers investigating the radial and latitudinal intensity gradients of ACRs and numerical solutions to the CRTE are in preparation. Notable consequences of the lower energy range studied here are that our intensity measurements at and below the ACR O spectral peak are unique during this period, and the outer heliospheric ACR H and He ions are measured at the lowest energies possible, below which solar or IP-accelerated particles dominate the signal. The 1993–1998 time-intensity profile of 2- to 5-MeV/nucleon IP ACR O at 1 AU is presented here for the first time, which, complimented by the time-dependent low-energy magnetospherically trapped ACR O observations of *Mazur et al.* [2000], extends the 7–27 MeV/nucleon magnetospherically trapped and IP ACR O time-intensity profiles of *Selesnick et al.* [2000] to a significantly lower energy. Since other investigations have focused on GCRs and higher-energy ACRs, this paper represents the first comprehensive analysis of the recovery of low-energy ACRs in the outer and inner heliosphere during the solar cycle 22 recovery phase. In addition to the analysis and discussion of sixteen independent ACR time-intensity profiles, including a single high-energy 1-AU IP ACR O time-intensity profile from *Selesnick et al.* [2000], we provide a simple parameterization of the data, which we use to quantify the forms of the recoveries, to study the dependence of the ACR recovery profiles on various physical quantities. This parameterization should be useful to those who may wish to conveniently compare this large set of ACR data to their models.

**Table 1.** Voyager 1 and 2 Spacecraft Positions[a]

| | Voyager 1 | | Voyager 2 | |
|---|---|---|---|---|
| Year[b] | Radius, AU | Latitude, °N | Radius, AU | Latitude, °S |
| 1991 | 45.4 | 31.5 | 34.9 | 3.4 |
| 1992 | 49.0 | 31.9 | 37.6 | 6.7 |
| 1993 | 52.7 | 32.3 | 40.5 | 9.5 |
| 1994 | 56.3 | 32.5 | 43.3 | 11.9 |
| 1995 | 59.9 | 32.8 | 46.2 | 14.1 |
| 1996 | 63.6 | 33.0 | 49.3 | 16.0 |
| 1997 | 67.2 | 33.2 | 52.3 | 17.7 |
| 1998 | 70.8 | 33.4 | 55.3 | 19.1 |
| 1999 | 74.5 | 33.5 | 58.4 | 20.5 |
| 2000 | 78.1 | 33.7 | 61.4 | 21.6 |

[a] Heliographic coordinates are used.
[b] Positions are for the middle of each year.

[5] In section 2 the spacecraft and instrumental details are presented before the various ACR H, He, and O time-intensity profiles are reported. In section 3 the four-parameter fitting function is described and justified and the methods and results of the parameterization procedure are reported, followed by a discussion of the dependence fitting parameters have on kinetic energy, rigidity, and mass. The discussion in section 4 presents the interpretation of the observed ACR recoveries that we judge is best supported by the observations. Section 5 summarizes the results and states the primary conclusions we have drawn.

## 2. Observations

[6] The Voyager 1 and 2 Spacecraft are receding from the Sun at 3.6 and 2.9 AU/year, respectively, as they travel through the distant heliosphere. Near the start of the recovery period, on the first day of 1992, V1 and V2 were situated at helioradii of 47.1 and 36.2 AU and heliolatitudes of 31.7°N and 5.1°S, and toward the end of the recovery, on

the first day of 2000, at 76.3 and 59.9 AU and 33.6°N and 21.1°S, respectively. Table 1 provides a yearly listing of the heliographic coordinates of the Voyager probes. In this work all of the Voyager observations are derived from measurements taken by the two nearly identical LECP instruments (one on each Voyager spacecraft), each of which is a dual aperture solid-state detector stack that makes dE/dx versus E and particle counting rate measurements [*Krimigis et al.*, 1977]. The two deep space probes return data from LECP that provide kinetic energy, composition, and differential intensity observations. Although anisotropy measurements and three minute time resolution are also possible, only omnidirectional and 26-day intensity averages are used throughout this paper, 26 days corresponding approximately to the effective solar rotation period experienced by V1 and V2. In addition, hundreds of separate background corrections, for each species, energy band, spacecraft, and year were carefully performed, using detailed pulse height analysis to ensure the accuracy of the LECP measurements [*Hill*, 2001]. These background corrections were significant only for the H data during the ~1992–1996 period. The resulting V1 protons (Figure 1), Voyager and 1-AU ACR O (Figure 2), and Voyager ACR H, He, and O (Figure 3) intensities are plotted from 1991 to 2000.

[7] For 1 AU comparisons, interplanetary measurements from the LICA sensor on SAMPEX are reported here, in addition to published observations from the SAMPEX, Advanced Composition Explorer (ACE), Wind, and IMP-8 spacecraft. The four previously published data points shown in Figure 2a are 3–4 MeV/nucleon IP ACR oxygen data from the LEMT instrument on the Wind spacecraft with times centered on 1995.55 [*Reames et al.*, 1997], 1995.61, and 1996.14 [*Cummings et al.*, 1997], and ACE/ULEIS measurements of 2–4 MeV/nucleon IP ACR oxygen centered on 1997.95 [*Christian et al.*, 1999]. Note that the 1995.55 and 1995.61 data points are so similar as to nearly appear as one symbol in Figure 2a. We calculated the five remaining 1 AU data points in Figure 2a from the same SAMPEX/LICA data used to construct the 1-AU ACR O spectrum reported by *Mazur et al.* [2000] (and compared with Voyager data by *Hill et al.* [2002]). The non-ACR contribution, such as solar energetic particles (SEPs) and ions from corotating interaction region (CIRs), was removed by fitting and subtracting the shock-accelerated power law portion of the annually averaged spectra. To avoid contamination of the IP signal from such solar, heliospheric, or magnetospheric particle sources, we use only the SEP/CIR-subtracted observations of 1.75- to 5.00-MeV/nucleon oxygen made while SAMPEX was at high geomagnetic latitudes, where IP ions are well observed, and use a quiet time criterion that the $^4$He flux be less than 0.02 $\mathrm{cm^{-2}\,s^{-1}\,sr^{-1}}$ $(\mathrm{MeV/nucleon})^{-1}$. Annual averages of the LICA oxygen measurements were used to mitigate against statistical limitations; however, the 1995 data point has nevertheless been omitted due to a prohibitively large statistical uncertainty. The LICA measurements (Figure 2a) add new lower-energy, time-dependent observations of IP ACR oxygen intensities to the ACE and SAMPEX higher-energy 7- to 29-MeV/nucleon O data reported by *Selesnick et al.* [2000] and shown here (Figure 2b) supplemented by the addition of the two earliest data points, which are from the IMP-8 spacecraft [*Mewaldt et al.*, 1993].

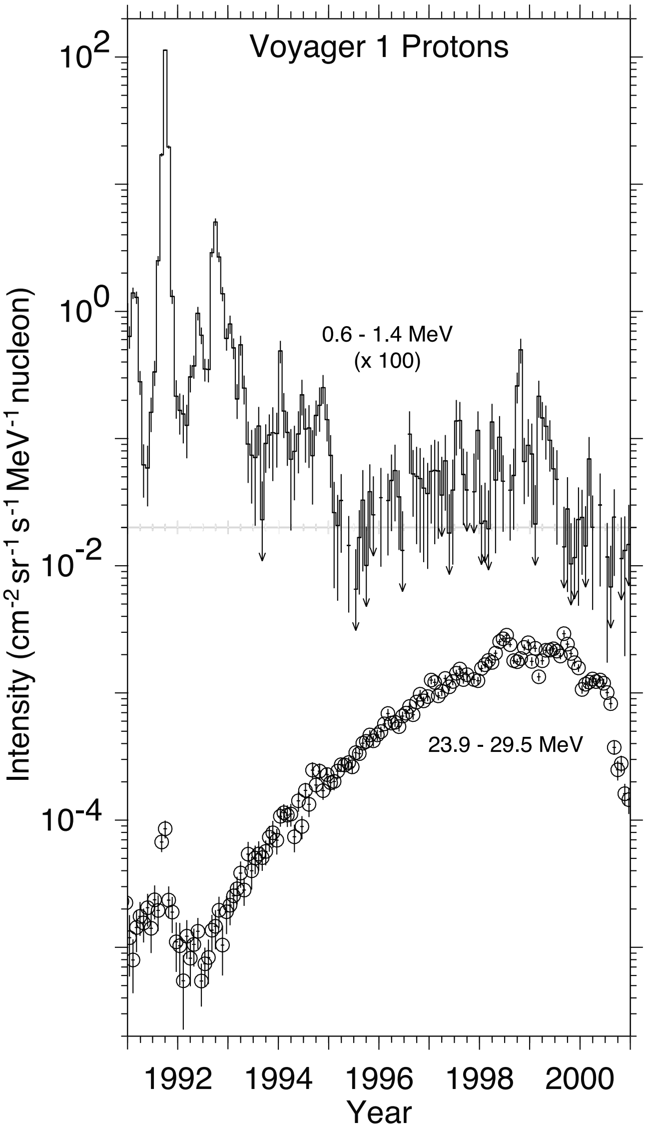

**Figure 1.** Intensities of 0.6- to 1.4-MeV and 24- to 30-MeV protons measured at Voyager 1 from 1991 to 2000 with the LECP instrument. The upper time-intensity profile (whose intensities are multiplied by 100) is dominated by solar energetic and interplanetary accelerated H, which is correlated with the level of solar cycle activity. The lower profile is almost entirely composed of anomalous cosmic ray H (except in 1991) and is roughly anticorrelated with the solar activity level.

[8] The energy ranges for V1 and V2 were selected to match the available SAMPEX/LICA energy band at the low energies and to match the published SAMPEX, ACE, and IMP-8 energy ranges at the higher energies. The low-energy oxygen energy ranges for the V1 and V2 LECP data are 1.00 to 4.05 MeV/nucleon and 0.95 to 4.78 MeV/nucleon, respectively, while the high-energy bands are 6.89 to 27.6 and 8.00 to 27.4 MeV/nucleon for V1 and V2, respectively. These Voyager observations, together with the 1-AU oxygen data, allow a simultaneous investigation into the energy- and time-dependence of ACR oxygen in the inner and outer heliosphere.

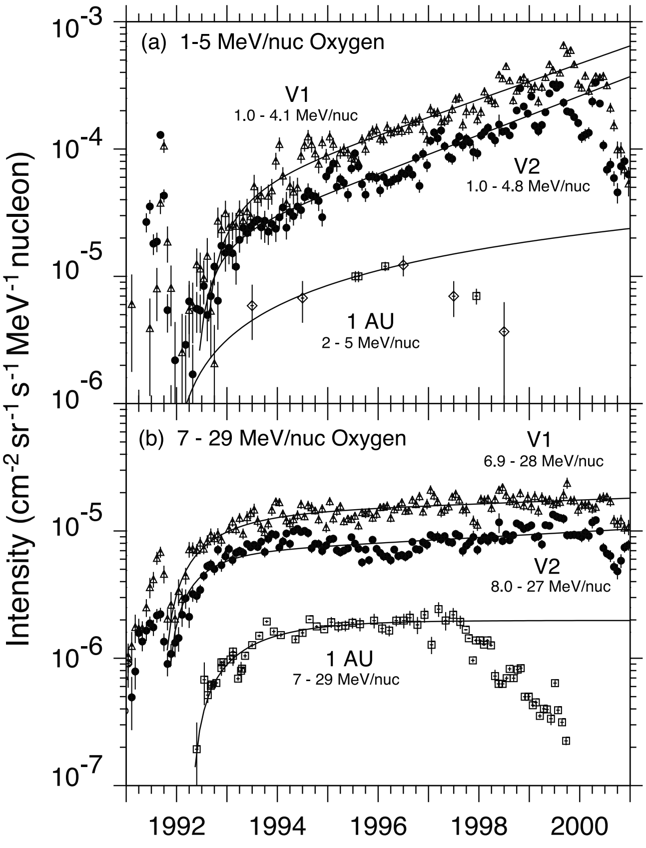

**Figure 2.** Intensities of (a) 1- to 5-MeV/nucleon and (b) 7- to 29-MeV/nucleon oxygen measured at Voyager 1 (triangles), Voyager 2 (circles), and at 1 AU (diamonds and squares) during 1991–2000. New measurements from the LICA sensor on SAMPEX (diamonds) are distinguished from the previously published 1-AU measurements (squares) described in section 2 [*Mewaldt et al.*, 1993; *Reames et al.*, 1997; *Cummings et al.*, 1997; *Christian et al.*, 1999; *Selesnick et al.*, 2000]. The solid curves represent fits (equation (1)) to the data as described in section 3, with fitting parameters listed in Table 2. Note that the fit curves are extrapolated beyond the actual fitting periods (Table 2), which were chosen to exclude periods of excessive interplanetary background or renewed solar modulation.

[9] After the solar cycle 22 maximum in 1989, solar activity waned until March and June of 1991 when the largest solar events of the cycle occurred. The cosmic rays, which had already begun to recover, were sharply modulated, with, for example, >70 MeV galactic cosmic rays in the outer heliosphere at Voyager 1, Voyager 2, and Pioneer 10 dropping to their lowest levels of the cycle in the latter half of 1991 [*McDonald et al.*, 1994]. The noted universality of large Forbush decreases associated with this renewed solar activity at widely separated spacecraft throughout the heliosphere, despite the localized nature of the initial active regions on the Sun, may be indicative of a global merged interaction region (GMIR), a phenomenon in which the coalescence of adjacent propagating interaction regions forms a large-scale disturbance that may encompass a large range of heliolatitudes and heliolongitudes at great distances from the Sun [*Burlaga et al.*, 1985]. Under these conditions the anomalous cosmic ray populations declined throughout the heliosphere and established a heliosphere comparatively free of ACRs; subsequently, anomalous ions began to repopulate the heliosphere as the disturbance moved beyond the termination shock. The recovery period from 1991.7 to the end of 1999, by excluding the earlier recovery that was truncated by the GMIR associated with the March/June 1991 events, allows a particularly neat comparison of the transport of ACRs of various species and at various heliospheric locations. Additionally, study of this recovery period benefits from the fortunate position of the Voyager spacecraft in the outer heliosphere, where SEP and IP-accelerated contamination is reduced and ACRs are dominant at the LECP energy range.

[10] In Figure 1 the time histories of both SEP/IP and ACR proton intensities are shown from 1991 to 2000 at Voyager 1. An examination of annually averaged H, He and O energy spectra from 1991 at both V1 and V2 (not shown) reveals distinct falling power law forms typically resulting from shock acceleration in the heliosphere [*Hill*, 2001]. These shock particles dominate the 1991 H and He spectra from ~0.5 to 20 MeV/nucleon and up to about 3 MeV/nucleon for O (in 1991, ACRs comprise most of the O spectrum above this energy, but do not contribute significantly to lower-energy O or to H and He within the LECP energy range). Through examination of these spectra, as well as the distinct time profiles, we determine that the 0.6 to 1.4 MeV energy band responds to SEP and IP-accelerated protons throughout the period of interest (Figure 1). In the same way, the intensities in the 24 to 30 MeV band are found to be due to ACR H, except for the small brief peak near 1991.7, which is due to the high-energy contribution of the power law shock spectrum resulting from the GMIR associated with the March/June 1991 particle events (Figure 1). The large amount of activity in the SEP/IP time series at the beginning of the recovery decreased considerably by 1993 and after 1994 solar minimum conditions were well established. At V2 (not shown) solar activity continued at higher relative levels for a longer period, and didn't subside until 1999. Moreover, there are enhanced proton intensities at V2 resulting from CIRs, particularly in 1994 [*Krimigis et al.*, 1997]. Despite these differences the overall behavior at V2 and at V1 (Figure 1) is similar from 1991 to 1999: a decrease in ~1 MeV proton intensities due to reduced solar activity, accompanied by recovering ACR H intensities. The increase in ACR intensities is presumably due to decreasing disturbance levels that reduce the amount of ACR scattering and allow the establishment of global drift patterns. This SEP/IP and ACR behavior is a manifestation of the familiar anticorrelation between cosmic ray intensities and solar activity indices.

[11] The ACR oxygen measurements we present were made in three heliospheric regions: at 1 AU in the ecliptic (SAMPEX, ACE, Wind, IMP-8), the outer heliosphere at northern heliolatitudes (V1), and the outer heliosphere at southern heliolatitudes (V2), while all of the ACR proton and helium observations are from the outer heliospheric spacecraft. In Figure 2 ACR oxygen intensities from each of the three regions, and for two energy ranges, are displayed as a function of time. Figure 2a shows low-energy 1- to 5-MeV/nucleon O at V1, V2, and 1 AU from 1991 to 2000, where data were available, and Figure 2b displays

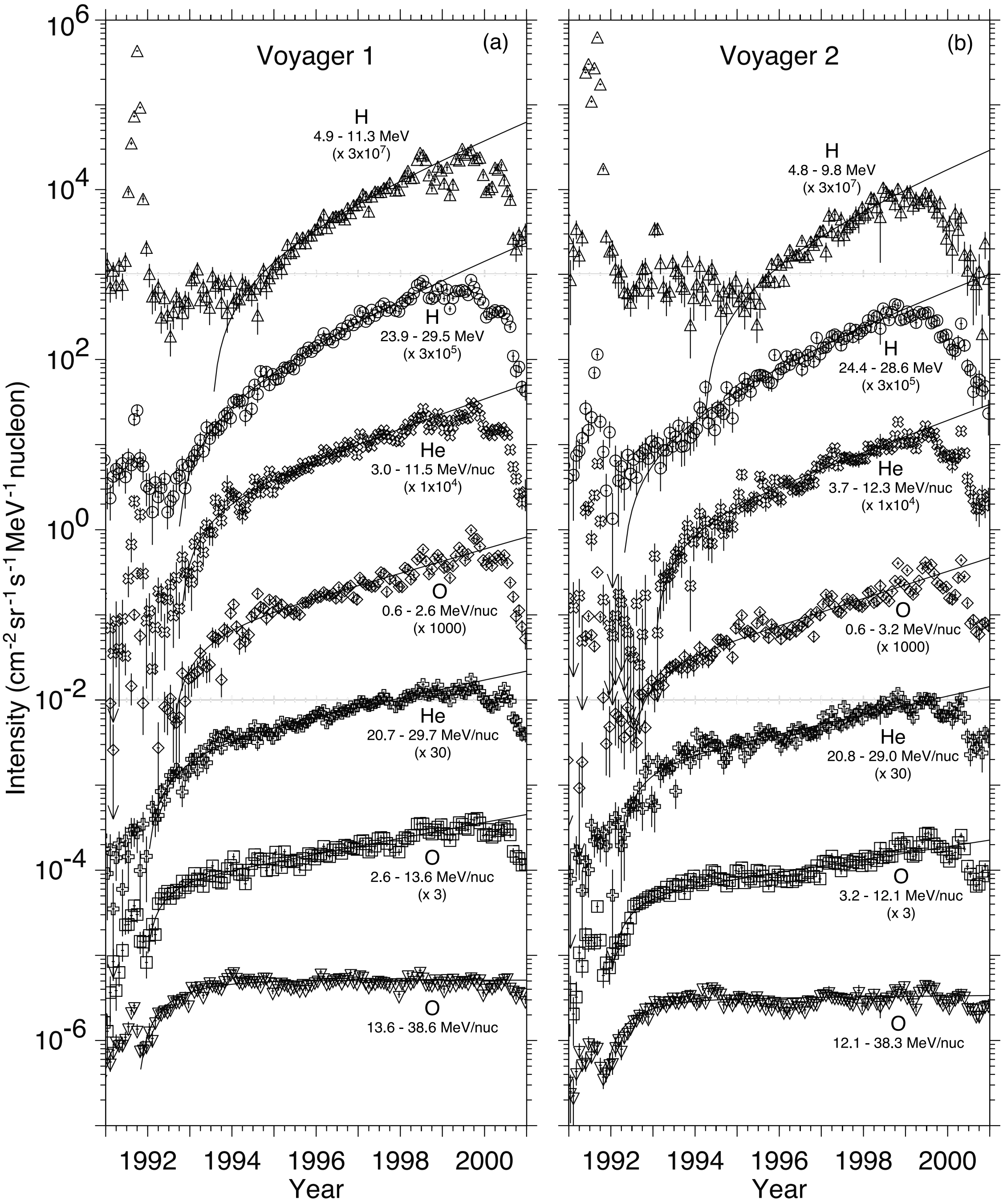

**Figure 3.** Intensities of H, He, and O from (a) Voyager 1 and (b) Voyager 2 during 1991–2000, covering a rigidity range from 100 to 4300 MV. For each time intensity profile the species, energy range, and multiplicative intensity offset is labeled. From top to bottom, the rigidities and species of the displayed particles are 120 MV H (upward triangles), 220 MV H (circles), 440 MV He (tilted crosses), 800 MV O (diamonds), 870 MV He (crosses), 1700 MV O (squares), and 3300 MV O (downward triangles), where singly charged ions have been assumed. The solid curves represent fits to the data, just as in Figure 2.

higher energy 7–29 MeV/nucleon O from the same three positions. After 1991.7 only ACR O contributes significantly to the intensities, while before this time there is a mixture of locally accelerated and anomalous ions.

[12] There are several important features of the ACR recovery that are displayed in Figure 2. During the initial recovery (IR) period, from 1991.7 to 1994.5, all of the ACR intensities underwent a similar recovery of the form $1 - e^{-t/\tau}$ (see equation (1)) where $t$ is time and $\tau$ is the time constant. This behavior cannot be detected for the low-energy 1 AU O data (Figure 2a) since the first measurement is not until 1993, after the onset of recovery. From 1994.5 to 1997.5, when solar minimum conditions prevail in the inner and outer heliosphere, the high-energy O intensities at all three helio-

**Table 2.** ACR Particle Properties and Recovery Profile Fit Parameters

| Species[a] and Space-craft Name | | Kinetic Energy Per Nucleon, MeV/nucleon | | | Total K.E., MeV | Magnetic Rigidity, MV | | | Speed | Intensity[c,d], Flux Units[e] | Initial Time[c], Years | Recovery Time[c], Years | Growth Time[c], Years | Fitting Period[c], Years |
|---|---|---|---|---|---|---|---|---|---|---|---|---|---|---|
| | | $E_{\mathrm{min}}$ | $E_{\mathrm{max}}$ | $E$[b] | $\mathcal{T}$ | $R_{\mathrm{min}}$ | $R_{\mathrm{max}}$ | $R$[b] | $\beta = v/c$ | $j_a$ | $t_i$ | $\tau$ | $T$ | |
| H | V1 | 4.993 | 11.34 | 7.52 | 7.52 | 97 | 146 | 119 | 0.13 | $1.9 \pm 0.9 \times 10^{-4}$ | 1993.50 ± 0.83 | 10.4 ± 5.6[f] | 2.44 ± 0.24 | ‘94.0–98.0 |
| H | V2 | 4.800 | 9.800 | 6.90 | 6.90 | 95 | 134 | 114 | 0.12 | $1.6 \pm 1.0 \times 10^{-4}$ | 1994.19 ± 0.98 | 13.4 ± 8.9[f] | 2.51 ± 0.55 | ‘95.0–98.5 |
| H | V1 | 23.91 | 29.50 | 26.6 | 26.6 | 213 | 237 | 225 | 0.23 | $4.8 \pm 1.4 \times 10^{-4}$ | 1992.67 ± 0.54 | 11.2 ± 3.6[f] | 2.40 ± 0.11 | ‘93.0–98.0 |
| H | V2 | 24.40 | 28.60 | 26.4 | 26.4 | 215 | 233 | 224 | 0.23 | $3.4 \pm 1.6 \times 10^{-4}$ | 1992.24 ± 0.99 | 17.1 ± 8.4[f] | 2.72 ± 0.18 | ‘93.0–99.0 |
| He | V1 | 2.986 | 11.48 | 5.85 | 23.4 | 300 | 589 | 420 | 0.11 | $1.9 \pm 0.2 \times 10^{-4}$ | 1992.74 ± 0.18 | 1.23 ± 0.21 | 2.49 ± 0.10 | ‘92.8–98.5 |
| He | V2 | 3.710 | 12.30 | 6.76 | 27.0 | 334 | 610 | 451 | 0.12 | $9.5 \pm 9.2 \times 10^{-5}$ | 1993.01 ± 2.50 | 1.11 ± 0.52 | 2.31 ± 0.28 | ‘93.1–98.5 |
| He | V1 | 20.65 | 29.74 | 24.8 | 99.2 | 792 | 952 | 868 | 0.23 | $8.2 \pm 1.5 \times 10^{-5}$ | 1991.95 ± 0.63 | 1.24 ± 0.31 | 4.13 ± 0.34 | ‘92.0–99.0 |
| He | V2 | 20.80 | 29.00 | 24.6 | 98.4 | 795 | 940 | 864 | 0.22 | $5.0 \pm 0.4 \times 10^{-5}$ | 1992.18 ± 0.19 | 0.69 ± 0.17 | 3.90 ± 0.22 | ‘92.2–99.5 |
| O | V1 | 0.646 | 2.643 | 1.31 | 21.0 | 557 | 1127 | 792 | 0.05 | $5.2 \pm 0.9 \times 10^{-5}$ | 1992.54 ± 0.53 | 0.97 ± 0.20 | 3.06 ± 0.16 | ‘92.5–99.0 |
| O | V2 | 0.600 | 3.170 | 1.38 | 22.1 | 536 | 1235 | 814 | 0.05 | $2.0 \pm 0.1 \times 10^{-5}$ | 1992.44 ± 0.17 | 0.68 ± 0.15 | 2.72 ± 0.08 | ‘92.5–99.0 |
| O | V1 | 2.644 | 13.57 | 5.99 | 95.8 | 1128 | 2562 | 1699 | 0.11 | $2.1 \pm 0.1 \times 10^{-5}$ | 1991.91 ± 0.08 | 0.52 ± 0.07 | 4.63 ± 0.11 | ‘91.9–00.0 |
| O | V2 | 3.170 | 12.10 | 6.19 | 99.0 | 1235 | 2418 | 1727 | 0.11 | $1.5 \pm 0.1 \times 10^{-5}$ | 1991.94 ± 0.08 | 0.61 ± 0.08 | 5.70 ± 0.24 | ‘91.9–99.0 |
| O | V1 | 13.57 | 38.56 | 22.9 | 366 | 2562 | 4347 | 3335 | 0.22 | $5.1 \pm 0.0 \times 10^{-6}$ | 1991.74 ± 0.27 | 1.00 ± 0.06 | $\infty$[g] | ‘91.8–00.5 |
| O | V2 | 12.10 | 38.30 | 21.5 | 344 | 2418 | 4332 | 3234 | 0.20 | $3.0 \pm 0.1 \times 10^{-6}$ | 1991.77 ± 0.08 | 0.84 ± 0.08 | 81.5 ± 42.3 | ‘91.8–00.5 |
| O | V1 | 1.00 | 4.05 | 2.01 | 32.2 | 693 | 1396 | 984 | 0.07 | $4.2 \pm 0.3 \times 10^{-5}$ | 1992.55 ± 0.14 | 0.80 ± 0.13 | 3.10 ± 0.10 | ‘92.5–99.0 |
| O | V2 | 0.95 | 4.78 | 2.13 | 34.1 | 676 | 1517 | 1012 | 0.07 | $1.8 \pm 0.1 \times 10^{-5}$ | 1992.37 ± 0.16 | 0.57 ± 0.13 | 2.84 ± 0.07 | ‘92.5–99.0 |
| O | 1AU | 2 | 5 | 2.2 | 35 | 690 | 1550 | 1040 | 0.07 | $2.4 \pm 2.8 \times 10^{-4}$ | 1991.83 ± 4.55 | 90 ± 110[f] | $\infty$[g] | ‘92.0–97.0 |
| O | V1 | 6.89 | 27.6 | 13.8 | 221 | 1822 | 3667 | 2583 | 0.17 | $1.3 \pm 0.0 \times 10^{-5}$ | 1991.72 ± 0.03 | 1.03 ± 0.06 | 29.5 ± 2.5 | ‘91.8–00.5 |
| O | V2 | 8.00 | 27.4 | 14.8 | 237 | 1964 | 3654 | 2677 | 0.18 | $6.5 \pm 0.2 \times 10^{-6}$ | 1991.78 ± 0.17 | 0.67 ± 0.05 | 19.8 ± 1.8 | ‘91.8–00.5 |
| O | 1AU | 7 | 29 | 14.3 | 229 | 1840 | 3760 | 2630 | 0.17 | $2.0 \pm 0.0 \times 10^{-6}$ | 1992.28 ± 0.54 | 1.21 ± 0.09 | $\infty$[g] | ‘92.0–97.5 |

[a] Singly ionized charge state is assumed.

[b] Geometric mean of the extrema.

[c] The recovery fit function is $j(t) = j_a(1 - \exp(-(t - t_i)/\tau))\exp((t - t_i)/T)$.

[d] Time asymptotic intensity of the recovery factor $j_a(1 - \exp(-(t - t_i)/\tau))$.

[e] Flux units are $\mathrm{cm}^{-2}\ \mathrm{sr}^{-1}\ \mathrm{s}^{-1}\ (\mathrm{MeV/nucleon})^{-1}$.

[f] Value has questionable significance due to IP background or lack of data during the IR phase.

[g] The growth factor $\exp((t - t_i)/T)$ was found not to be necessary for these fits.

spheric positions (Figure 2b) increased only slightly, by about 18%. At a somewhat higher energy range, 13–38 MeV/nucleon, the oxygen intensities are even more strikingly constant for many years following the IR period (Figure 3). During the 1994.5 to 1997.5 period the low-energy ACR O intensities (Figure 2a) are increasing at a high rate, with the Voyager intensities showing the beginning of exponential growth that continues to the end of 2000. The low energy 1-AU intensities may have doubled during the 1994.5 to 1997.5 period, but the relatively large error bars on the 1993 and 1994 data points make a conclusive determination difficult. Finally, during the 1997.5 to 2000.0 period, there are three distinct behaviors (Figure 2). The low-energy outer heliospheric intensities continue to increase exponentially, the high-energy outer heliospheric intensities are relatively constant, and the inner heliospheric ACR fluxes decrease markedly, at low and high energies, due to the increasing solar cycle 23 activity.

[13] In Figure 2, ACR oxygen ions of only two energy ranges are shown. To examine the energy dependence of the ACR recovery profiles in more detail, we show in Figure 3 the intensities of H, He, and O ions versus time for ACRs of seven magnetic rigidities ranges, from 100 to 4300 MV and with kinetic energies ranging from 0.6 to 39 MeV/nucleon. Table 2 lists the properties of the species and energies of ACRs that we discuss in this paper. In Figure 3 the Voyager 1 and 2 ACR data include two energy ranges each for H and He, along with three different O energy ranges. Since the two energy ranges of O used in Figure 2 were specifically selected to match the SAMPEX/LICA and published 1-AU data, the three energy ranges used in Figure 3 differ from and overlap with the Figure 2 energy ranges. To facilitate a visual comparison of the relative shapes of the recovery profiles, convenient multiplicative factors (indicated in Figure 2) are employed to offset the time-intensity profiles with respect to one another.

[14] Significant features of the Voyager 1 and 2 ACR recovery profiles shown in Figure 3 are the similarity of the IR period, before 1994.5, and the variety of the rigidity-dependent exponential growth rates of the late recovery (LR), or growth phase, from 1994.5 to 2000.0. As is discussed in detail in section 3, the ACR recovery is similarly prompt for each of the time series shown, with He and O having similar time constants, and the proton behavior being obscured by interplanetary background. All of the ACR intensities increased by an order of magnitude during the first couple years of the recovery. Also studied in section 3 is the striking exponential growth displayed by the lower-energy ACR intensities after mid 1994, with the He and O recovery profiles well represented by simple exponentials for nearly six years. ACRs having the lowest rigidities have the shortest *e*-folding times, down to a minimum of 2.3 years, and the highest rigidity ACR O intensities, at about 3 GV, are quite constant at both spacecraft for over 6 years, corresponding to an effectively infinite time constant. Here, unlike during the IR period, there is a range in the magnitude of intensity increase from no increase to an order of magnitude increase, largely ordered by rigidity. The similarity of the intensity profiles of the ACR species shown during the IR period, followed by the different, but well-ordered, simple behavior of the ACR intensities during the LR period suggests that two distinct physical mechanisms are at work, each separately dominating the recovery either before or after mid 1994.

The likely cause for these two distinct periods of ACR behavior is discussed in section 4.

[15] Another striking feature of the ACR O time histories at both low and high energies (Figure 2) is the large delay between the onset of renewed modulation at 1 AU and that in the outer heliosphere. For high-energy oxygen (Figure 2b) there is no sign of significant large-scale modulation at V1 or V2 until the second half of 2000, despite a rapid drop at 1-AU beginning in the second half of 1997. ACR O with an energy range of 13 to 38 MeV/nucleon at V1 and V2 (Figure 3) shows no sign of renewed modulation through the end of 2000. As with the high-energy data, the low-energy O intensity at 1 AU (Figure 2a) drops noticeably in 1997 and continues to do so in 1998, while the outer heliospheric, low-energy anomalous oxygen intensities do not decrease significantly until late 1999.

[16] These facts indicate a large-scale modulation lag time of $\sim$2.5 years between the inner and outer heliosphere, showing that modulation is much less effective in the outer heliosphere, although this region may respond to some shorter term ($\sim$150 day) solar variations, as discussed by *Hill et al.* [2001b]. The large, factor of $\sim$10 increase in the V1 and V2 low-rigidity ACR intensities from 1994 to 2000 (Figure 3) might therefore be explainable by a significant spatial effect resulting from the spacecraft moving through a relatively stable spatial structure with a significant radial intensity gradient. This view appears to require substantial disturbances in the IP medium, perhaps resulting from the heliomagnetic polarity reversal, before the outer heliospheric spatial structure, and perhaps the TS source itself, is disrupted and eventually rapidly brought out of equilibrium, resulting in a comparatively sudden intensity decrease like that observed in the last half of 2000. Through 2000, the continued modest modulation of high energy oxygen intensities (Figure 2) and lack of modulation above 13 MeV/nucleon (Figure 3) could indicate that the ACR source spectrum at these higher energies is still relatively stable even as solar maximum approaches and that the solar disturbances are still too weak as of 2000 to significantly impede the high-rigidity particles from gaining access to the outer heliosphere. This would mean that the portion of the outer heliospheric ACR spectrum above about 13 MeV/nucleon [*Hill et al.*, 2002] represents the ACR source spectrum itself, with intensity differences between V1 and V2 attributable to latitudinal (and longitudinal) variations in the source distribution, presumably at the termination shock. *Stone et al.* [1996] have also suggested that the small change in 7.1- to 17.1-MeV/nucleon ACR O may indicate very little difference between the source and observed intensities.

## 3. Parameterization

[17] To facilitate a quantitative understanding of the behavior of the ACR intensities during the recovery phase, it is useful to parameterize the ACR time-intensity profiles. Then we can study the dependence various parameters have on particular physical quantities relevant to transport theory, with the intent to seek an organizing pattern that could provide insight into the physics of cosmic ray transport. Another useful result of systematically fitting the numerous ACR recovery profiles with simple four-parameter fit functions is to provide to theoretical modelers and others a handy set of functions with which an easy comparison between predictions and observations can be made. In addition to a set of simple fits, each with a small number of parameters, as we pursue here, it is also possible to use a single, more complicated fit function with many parameters to simultaneously probe the phenomenology of all of the ACR H, He, and O recovery profiles, as was done by *Hill* [2001].

[18] The general form of the time-intensity profiles in Figures 2 and 3 is that of an initial recovery phase followed by an exponential growth phase. The intensity variation during the recovery period of solar cycle 22 has been successfully represented for GCRs and higher-energy ACRs by a function of the form $1 - \mathrm{e}^{-t/\tau}$ [*McDonald et al.*, 2000b, 2002]. In Figures 2 and 3 the striking exponential growth of the intensity in the outer heliosphere after 1994 is sustained over the rest of the recovery phase, until renewed solar activity increases the level of modulation in 2000 and 2001. For approximately 5 years of the recovery, the oxygen and helium data are well represented by linear fits to the logarithm of intensity, i.e., exponential growth. Why these anomalous cosmic ray intensities take on a distinct and sustained exponential growth form rather than the $1 - \mathrm{e}^{-t/\tau}$ recovery form predominantly observed for GCRs and higher-energy ACRs during cycle 22 is an important topic addressed in this paper and in detail by *Hill* [2001] and is related to the effects of spacecraft motion. For protons the interpretation is more difficult, due largely to IP background, as discussed below; however, at this point we merely wish to parameterize the behavior, most of the physical interpretation being postponed until section 4. Combining the $1 - \mathrm{e}^{-t/\tau}$ recovery factor with an exponential growth factor, we arrive at the function,

$$j(t) = j_{\mathrm{a}}\left(1 - e^{-(t-t_{\mathrm{i}})/\tau}\right)e^{(t-t_{\mathrm{i}})/T}, \qquad (1)$$

where $j_{\mathrm{a}}$ is the time-asymptotic intensity value of the initial recovery factor, $\tau$ is the *e*-folding recovery time of the initial recovery factor, $t_{\mathrm{i}}$ is the initial time defined by $j(t_{\mathrm{i}}) = 0$, and $T$ is the *e*-folding time of the late recovery exponential growth factor $\exp((t - t_{\mathrm{i}})/T)$. This functional form reduces to that used by *McDonald et al.* [2000b, 2002] when $T$ approaches infinity.

[19] We list in Table 2 the fit parameters for the twenty ACR recovery profiles shown in Figures 2 and 3. A $\chi^2$ minimization procedure was performed on 26-day-averaged data that were smoothed with 1-year running averages since it is only the long-term features that are of interest here; shorter-term variations were discussed by *Hill et al.* [2001b]. In a few cases "edge-effects" from the smoothing routine resulted in poor fits and the unsmoothed data were fit instead. In Figures 2 and 3 the fits were made to data from the recovery period only; therefore, periods of increasing modulation, significant background, or enhanced interplanetary acceleration were avoided (the fitting periods are listed in Table 2). For instance, the 4.8- to 9.8-MeV proton data from Voyager 2 in Figure 3b clearly show evidence of increasing modulation by 1998.5, and before about 1995 the interplanetary particle background prevents detection of the anomalous component. Regardless of the limited fitting

periods, the curves are extrapolated both forward and backward in time to better display the features of the recovery and to facilitate comparison.

[20] The fit to the low-energy 1-AU data (Figure 2a) is merely suggestive and has been done for completeness; clearly a varied family of curves could fit these data nearly as well. All of the oxygen and helium data are robustly represented by equation (1). That is, the resulting fit parameters (particularly $\tau$ and $T$) are relatively insensitive to reasonable choices of initial fitting values, owing to the quite distinct initial recovery before mid-1994 and exponential growth phase after mid-1994 evident in the data. The proton recoveries were more difficult to fit because the final fit parameters, especially $\tau$, were relatively sensitive to initial parameter estimates. The H exponential growth time $T$ was less sensitive than $\tau$, but none of the proton fit parameters was as robust as the analogous O and He parameters. The reason for this may simply be that the proton "initial" recovery period is longer, and the exponential growth phase is less well defined than for the other species, making it difficult to distinguish the two periods. Another reason, however, is that low-energy anomalous protons are undetectable above the locally accelerated proton background before about 1995, further complicating the fitting since the initial recovery data could not be included in the fitting period (which means that the $\tau$ parameter for protons is of questionable significance).

[21] The temporal parameters $t_i$, $\tau$, and $T$ are plotted against rigidity in Figure 4. With the exception of protons and the 2- to 5-MeV/nucleon 1 AU oxygen data (for which the relevant initial recovery measurements are non-existent), the $e$-folding recovery time $\tau$ is about one year for all of the ACRs, while the exponential growth constant $T$ ranges widely in a rigidity-dependent manner. This suggests that two different processes are dominating the IR and LR phases, respectively. Also, there is nearly a 1 year delay between the end of the initial recovery for outer and inner heliospheric 7- to 29-MeV/nucleon ACR O, where the quantity $t_{rec} = t_i + \tau$ is used to measure the transition from the initial recovery to the late recovery period. The fit function's recovery factor $1 - \exp(-(t - t_i)/\tau)$ is 0.63 when $t$ equals $t_{rec}$. The value of $t_{rec}$ for 7- to 29-MeV/nucleon ACR O is 1992.75 ± 0.07 at V1, 1992.45 ± 0.18 at V2, and 1993.49 ± 0.55 at 1 AU, making the difference $\Delta t_{rec}$ between the outer and inner heliosphere 0.89 ± 0.56 years. This means that the initial recovery phase ends first in the outer heliosphere and then in the inner heliosphere, just as one would expect from diffusion theory with a source at the TS. What is puzzling is that the onset of recovery (Table 2) is not earlier in the inner heliosphere for 7- to 29-MeV/nucleon ACR O intensities ($t_i$ = 1992.28 ± 0.54, 1991.78 ± 0.17, and 1991.72 ± 0.03 at 1 AU, V2, and V1, respectively), as one might have expected for an expanding region of easier diffusion originating at the Sun. This feature was also seen by *McDonald et al.* [2002] in 8- to 18-MeV/nucleon ACR O and 150- to 380-MeV/nucleon GCR He.

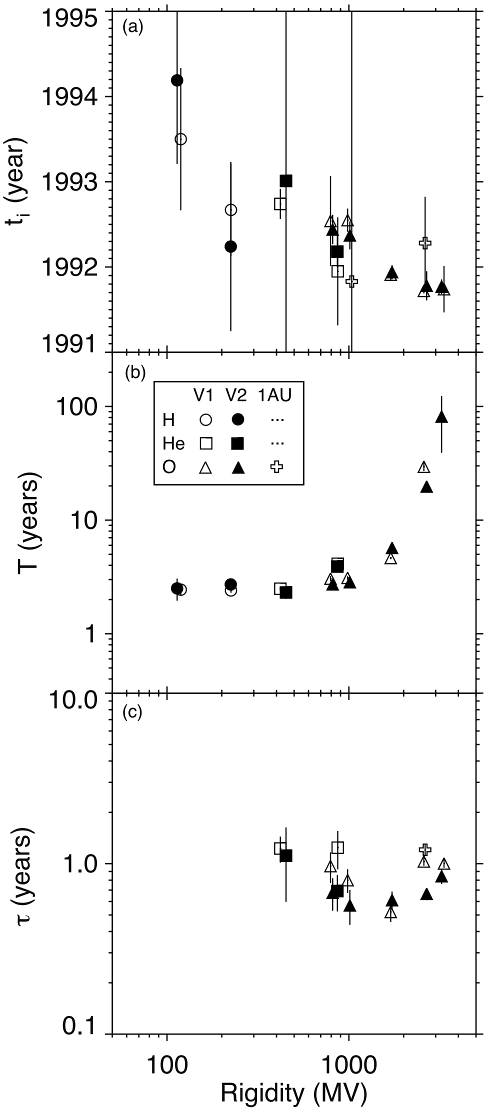

**Figure 4.** Temporal parameters (a) $t_i$, (b) $T$, and (c) $\tau$ from the ACR recovery fitting function (see equation (1) and Table 2), plotted versus rigidity. The legend in Figure 4b describing the plotting symbols (which indicate both species and spacecraft) applies to Figures 4a and 4c as well. (b) Three ACR O recovery profiles have no plotted value for $T$, since the exponential growth factor was not found to be necessary to fit the data (i.e., $T = \infty$). (c) The ACR H time constants are omitted due to the large amount of interplanetary background during the initial recovery period, and the time constant for 2- to 5-MeV/nucleon O at 1 AU was also omitted since there are too few early data points for a meaningful determination of $\tau$.

[22] The dependence of the fit parameters upon ACR particle properties can shed light on the underlying physics. We have examined the three temporal fit parameters $t_i$, $\tau$, and $T$, and two derived quantities $(\partial \ln j/\partial t)^{-1}$ and $t_{rec}$ as functions of four ion properties, $E$ (kinetic energy per nucleon), $\mathcal{T}$ (total kinetic energy), $R$ (magnetic rigidity), and $A$ (mass number). The energy $E$ is uniformly poor at organizing the parameters, and $A$ is inferior to $R$ and $\mathcal{T}$, as it tends to exhibit an envelope with a significant spread. The quantities $R$ and $\mathcal{T}$ each ordered the data about equally as well, with $R$ displaying somewhat less scatter than $\mathcal{T}$ for the $t_i$, $\tau$, $(\partial \ln j/\partial t)^{-1}$, and $t_{rec}$ parameters. In Figure 4 we show only the dependence of $t_i$, $T$, and $\tau$ on rigidity, where the symbols additionally identify the species and spacecraft

associated with each measurement, as shown in the legend in Figure 4b. In Figure 4a the initial time parameter $t_i$ is plotted. Although the low-intensity measurements near $t_i$ are difficult, this parameter allows a meaningful comparison of the start of recovery for different ions. Were one to alternatively base the start of recovery upon the first indication of elevated ACR flux alone, for example, the times could be skewed by factors not directly related to cosmic ray physics, such as instrumental background levels and coincident IP particle events; therefore $t_i$ is preferred. The middle panel (Figure 4b) contains a plot of the exponential growth *e*-folding time $T$ versus $R$. The time $T$ is associated with the spatial intensity gradient of the particles [*Hill*, 2001], but putting that aside for the time being, $T$ is simply related to the time-asymptotic rate of increase of the anomalous component before the end of the recovery phase. Below bout 1000 MV the $T$ values are nearly independent of rigidity with a minimum value of 2.3 years, corresponding to an intensity doubling time of around 19 months. The recovery time $\tau$ is plotted in Figure 4c, indicating the characteristic time-scale of the initial recovery factor $1 - \exp(-(t - t_i)/\tau)$, which, it is argued by *Hill* [2001], is related to the recovery time one would expect if the spacecraft position were held constant. Note that the 7- to 29-MeV/nucleon ACR O values for $\tau$ (Table 2) are similar to the 1.0, 0.93, and 1.0 year time constants determined by *McDonald et al.* [2002] for 8- to 18-MeV/nucleon ACR O at V1, V2, and 1-AU, respectively.

[23] Overall, the time parameters tend to be about equally well organized by rigidity as by total kinetic energy, with $R$ perhaps slightly preferable to $\mathcal{T}$ in most instances. This similarity is not surprising if a power law-dependent scattering mean free path $\Lambda \propto R^{\eta}$ has an index $\eta$ near unity [*Hill*, 2001; *Hill et al.*, 2002] because then the diffusion coefficient $\kappa = v\Lambda/3$ would be proportional to $\mathcal{T}$. One significant feature of these parametric results is that the recovery profiles of these particles, with mass numbers ranging from 1 to 16, at heliospheric positions between 1 and 80 AU from the Sun, and with rigidities spanning from $\sim$100 to over 4000 MV, are nonetheless similar in form, generally varying from one another in an understandable, organized fashion. This suggests, from a physically based phenomenological standpoint, that it is possible to model the transport of the anomalous cosmic ray recovery systematically so as to understand the dependence that detailed features of these phenomena have on known physical quantities. A phenomenological modeling of this sort was undertaken by *Hill* [2001]. Perhaps the most surprising result illustrated by Figure 4 is that $\tau$ is not correlated with rigidity, since all of the values clustered around 1 year, while $t_i$ does exhibit a rigidity dependence. Our expectation was that the start of the ACR recovery, at a given heliospheric position, would be about the same for all rigidities, corresponding to the time when the transport properties of the interplanetary medium change near the Sun and propagate with the solar wind to the various heliospheric spacecraft. Moreover, it seemed reasonable to expect that the time constant $\tau$ would have been sensitive to particle rigidity, since a high rigidity particle should be able to diffuse in rapidly, with a short time constant, while a low rigidity particle should diffuse in slowly with a long time constant. However, it is neither $\tau$ nor $t_i$ but the growth time $T$ that is most clearly ordered by particle property, namely the rigidity. In section 4 we discuss the reason for this.

## 4. Discussion

[24] In this and a previous paper [*Hill et al.*, 2002] we have set out to report the unique ACR measurements from the Voyager 1 and 2 LECP instruments and the LICA sensor on SAMPEX and to set these observations in the context of a physical interpretation, based in transport theory. In future papers we will report and address the ramifications of intensity gradient calculations, make quantitative comparisons of the data with a numerical solution to the Fokker-Planck equation, and model the ACR recovery in a comprehensive, phenomenological manner [*Hill*, 2001]. We now discuss an interpretation of the observations herein, focusing on the ACR recovery period, but touching on solar modulation features as well.

[25] In section 3 the form of the inner and outer heliospheric ACR time-intensity profiles from the 1991–1999 recovery period has been examined (equation (1)) and parameterized (Table 2). At a minimum, an acceptable interpretation of these data (Figures 2 and 3) must explain (1) the distinct difference between the pre-1994 initial recovery of the form $1 - e^{-t/\tau}$ and the post-1994 exponential growth of the form $e^{t/T}$, (2) the similar $\sim$1 year time constants $\tau$ during the initial recovery period, at all rigidities, and (3) the substantial rigidity dependence of the exponential growth constant $T$ during the late recovery period. Unless accompanied by a supporting theoretical development, such an interpretation should also be (4) as simple as possible, (5) consistent with the physics of particle transport, as presently understood, and (6) consistent with other known observations.

[26] The Voyager observations of ACR recovery in the outer heliosphere during solar cycle 22 can be understood in a straightforward manner when divided into the IR (1991.7 to 1994.5) and LR (1994.5 to 2000.0) periods. We suggest that the intensity variations during the IR period are predominantly controlled by temporal variations arising from the rapid changes in the transport properties of the IP medium, that the LR observations are explained by the motion of the Voyager probes through a region of the heliosphere with spatially varying ACR intensities during a relatively unchanging solar minimum period, and that the mid-1994 transition from IR to LR can be explained by the evolution of the heliosphere to a state of near-equilibrium at that time.

[27] After the ACR population was substantially reduced throughout the heliosphere in 1991 and the IP disturbances or GMIR propagated beyond the ACR source region, presumably at the TS, the transport of ACRs from the TS toward the inner heliosphere began. The transport process is largely diffusive during the IR interval, including important convective and adiabatic cooling effects. As ACRs enter the heliosphere there is a rapid recovery throughout, with ACR intensities increasing by an order of magnitude during an approximately 2-year period. The precise recovery profile associated with the transport of ACRs into a nearly empty heliosphere is influenced by the relaxation time, i.e., the time, due to transport processes alone, that would be required for the distribution of ACRs in the heliosphere to

come into equilibrium following a discrete change in the IP transport properties. The recovery profile is further influenced by any prolonged (solar cycle) time dependence in the variation of the IP transport properties. That is, if the transport properties originating at the Sun change effectively instantaneously on the time-scale considered here, then the relaxation time alone would drive the temporal characteristics of the recovery profile at a given heliospheric position, whereas if the IP properties themselves vary over an interval significantly larger than the relaxation time, then these solar cycle variations would predominate. In both cases a time lag for the changing IP properties to propagate to a given heliospheric position would only be readily apparent when comparing recovery profiles from more than one position.

[28] The relaxation time or the solar cycle time dependencies need only account for the recovery profiles during the initial recovery period when all of the ACRs show similar $1 - e^{-t/\tau}$ forms with comparable time constants $\tau$ of about one year (Table 2). The similarity of the time constants $\tau$ suggests that it is the solar cycle dependence of the changing properties of the IP medium, and not the relaxation time, that is primarily responsible for ACR intensity variations during the IR period. This is because, based on numerical simulations [*Hill*, 2001] and simple analytical calculations, the relaxation time would be expected to depend significantly on rigidity, if, as expected, the mean free path length is *R* dependent, with higher-rigidity particles recovering more quickly and lower-rigidity particles recovering more slowly. Additional evidence that the cause of the initial recovery profiles of the outer heliospheric ACRs is indeed a predominantly temporal one comes from the 1-AU measurements, since the high-energy ACR O also shows a similar recovery profile to that in the distant heliosphere with a comparable time constant. Since, obviously, the Earth, unlike the Voyager spacecraft, is not moving out to more distant radii, this behavior at 1 AU is not spatial.

[29] With the end of the initial rush of ACRs repopulating the heliosphere during the IR period, the outer heliosphere approached a state of near equilibrium by mid-1994, as evidenced in part by the 6-year period of nearly constant ACR O fluxes above 13 MeV/nucleon. Why then, during this LR phase, do the lower rigidity ACR intensities, nonetheless, continue to increase in an exponential fashion, (as the parameterization study of section 3 shows)? The reason is that the Voyager spacecraft, as they approach the ACR source, are moving at radial velocities of about 3 AU/year through a radial intensity gradient that is positive and sizable for the lower energy ACRs. As is well known, an exponential form is precisely the prediction for the radial dependence of the ACR intensity using both simple convection/diffusion (which is not a poor approximation in the outer heliosphere) and the so-called force field solution [*Gleeson and Axford*, 1968]. Sophisticated numerical modeling of ACR transport and modulation using simulations dependent on radius, latitude, rigidity, and time [e.g., *Steenberg*, 1998] also provides ample examples of radial intensity profiles with exponential or near-exponential forms for large portions of the heliosphere. Moreover, the numerical modeling of *Hill* [2001] even found a close quantitative agreement between the observed and predicted rate of intensity increase using a time-dependent, spherically symmetric solution to the CRTE [*Hill*, 2001]. A rigidity dependence of the exponential time constant *T* with high-rigidity ACRs having nearly zero radial gradients, and low-rigidity ACRs having large, positive, radial gradients, as is observed, is just what would be expected if the scattering mean free path increased with rigidity, as has been frequently assumed and was found, e.g., by *Hill et al.* [2002]. We did not expect that *T* would be nearly independent of *R* below 1000 MV (Figure 4b), so this fact may provide additional insight concerning the spectrum of turbulence in the interplanetary magnetic field. Very small positive radial gradients have been found for ACR O at the higher energy ranges (above ~10 MeV/nucleon) by previous observational investigations [*Cummings et al.*, 1995; *McDonald et al.*, 1998]. Substantial positive radial gradients for the lower-rigidity ACRs and near zero radial gradients for high-energy ACRs have been calculated [*Hill*, 2001] using three methods, all found to be in agreement: an intensity gradient calculation, a phenomenological model, and the aforementioned numerical modeling.

[30] A quasi-equilibrium was also suggested by *Stone et al.* [1996] for as early as the 1993–1994 period, based largely on small intensity increases they observed in the V1 2.4 GV ACR O, but they attribute the increasing intensity of 0.7 GV ACR He to continued decreasing modulation. We agree that a near-equilibrium has been established before the end of 1994, but we feel that from mid-1994 to 1999 the equilibrium condition does not exclude the lower rigidity ACRs and that the dominant cause for the continued low-rigidity ACR intensity increases is not a temporal variation such as decreasing modulation, but a result of spacecraft motion through positive radial intensity gradients. Although the 7- to 29-MeV/nucleon ACR O intensities at 1 AU (Figure 2b) change very little after the initial recovery, the 2- to 5-MeV/nucleon 1-AU O intensities do increase. How is this consistent with the nearly static conditions that we suggest had come about in 1994? Modeling of ACR transport [*Steenberg and Moraal*, 1996; *Hill*, 2001] shows that the relaxation time for inner heliospheric ACRs at a given rigidity, should be longer than that of outer heliospheric ACRs. This means that the solar-cycle driven variation of the IP transport properties that determines the initial recovery timescale in the outer heliosphere (due to a much shorter relaxation time) could be replaced by the much longer relaxation time in the inner heliosphere. However, given a relatively unchanging ACR source spectrum at the TS, modeling suggests that higher-energy ACRs at 1 AU would still be expected to relax and approach the asymptotic intensity more rapidly than lower-energy ACRs [*Hill*, 2001], which would explain the smaller higher-energy intensity increase at 1 AU, after 1994.

[31] Measurements [*Hill et al.*, 2002] and numerical modeling [*Hill*, 2001] of the ACR spectra also support our interpretation. During the dominantly temporal IR period, both the data and the model showed a distinct, rapid shift of the energy of peak ACR intensity (e.g., the observed ACR O peak shifted from 9 to 1.3 MeV/nucleon). The rapid peak shift is a strong temporal feature of the model, which, as with the data, slowed considerably once the equilibrium conditions developed. During the LR equilibrium period, when the observed spectral peak energies were nearly

unchanging, the numerical model also showed very slowly shifting peak energies. These clearly observed and modeled spectral features add another layer of evidence for this interpretation.

[32] Our interpretation satisfies the six requirements at the beginning of section 4 and is also quantitatively supported by a time-dependent numerical model of ACR transport [*Hill*, 2001]: (1) The dual IR and LR form of the recovery arises naturally from the development of a near-equilibrium during 1994. (2) The unexpected similarity of the time constants $\tau$ follows if the IP transport properties change from solar maximum to minimum conditions in about 1 year and the relaxation time is shorter, which is consistent with the modeling of *Hill* [2001]. (3) The rigidity dependence of the exponential growth parameter $T$ is a natural consequence of the positive radial gradients expected from theory and modeling. (4) The interpretation is manifestly simple, requiring only that IP transport properties change and that an equilibrium develops. (5) The physics draws entirely from the generally accepted transport phenomena, diffusion, adiabatic cooling, convection, and drift, although drift is found to play a relatively minor role [*Hill*, 2001] in the outer heliosphere. (6) Other observations [e.g., *Stone et al.*, 1996; *McDonald et al.*, 2002] are all at the higher end of the energy range considered here, agree well with our measurements, and do not conflict with the interpretation we have given.

[33] Since our present course of investigation has focused on the recovery period of solar cycle 22, we do not here propose an interpretation of the ACR intensity data during modulation periods in the inner and outer heliosphere, but since the data do exhibit interesting solar modulation effects, we will specify the observations that require explanation. A suitable physical interpretation must account for the delay of ~2.5 years from 1997 to 2000 in the onset of large-scale modulation at 1 AU and the outer heliosphere (Figure 2), the sharply modulated low-energy outer heliospheric intensities, once modulation does occur (Figure 2a), and the modest high-energy outer heliospheric modulation in 2000 (Figure 2b). These three essential observations are broadly consistent with the plausible concepts that the effects of solar modulation will weaken with distance from the Sun, that the Voyager spacecraft are perhaps quite near to the ACR source region in 2000, and that the heliomagnetic polarity reversal, or some other global, solar-cyclic change could be an important factor in low-rigidity ACR transport, even in the outer heliosphere near the ACR source. The 2.5 year delayed modulation does not seem to support the interpretation of a step-function-like modulation barrier propagating outward at roughly the solar wind velocity, since that propagation speed would lead to a delay of less than 1 year. This is clearly a topic worthy of additional effort.

## 5. Conclusions

[34] From 1991 to 1999 outer heliospheric ACR H, He, and O intensities increased by one to two orders of magnitude (Figure 3) as interplanetary conditions changed from maximum to minimum levels of solar cycle activity, while inner heliospheric ACR O intensities grew until 1997 (Figure 2) when the period of increasing solar modulation commenced. Although qualitatively, ACR H recovers similarly to the other low-rigidity ions, the locally accelerated ion background that obscures the ACR H measurement until ~1995 limits the usefulness of the parametric study of the protons. We have found, however, that 0.6 to 39 MeV/nucleon (300 MV to 4.3 GV) outer heliospheric ACR He and O from late-1991 to mid-1994 exhibited an initial recovery of the form $1 - e^{-t/\tau}$ that was similar at all rigidities, with all species having *e*-folding time constants $\tau$ of about 1 year (Table 2) and an overall increase of about an order of magnitude. Inner heliospheric 7–29 MeV/nucleon (2.6 GV) ACR O had a very similar $\tau$ but the lower-energy 1-AU O data are not available before 1993, making a meaningful determination of $\tau$ impossible. Later, for the outer heliospheric recovery, after 1994, the similarity ceases; the lowest-rigidity ACR He intensities grew exponentially with a doubling time of 19 months, resulting in an order of magnitude increase from mid-1994 to 1999, during which period the highest-rigidity ACR O intensities were essentially constant. The recovery of intermediate rigidities varied smoothly between the two extremes. The high-energy 1-AU measurements of ACR O intensities from 1994 to 1997 are similar to those of Voyager 1 and 2.

[35] The most probable interpretation of these distinct observations is that the initial recovery period before mid-1994 corresponds to the temporal phase of the recovery, during which the intensities reflect the timescale associated with the time-dependence of the transport properties of the interplanetary medium as conditions evolve from a disturbed solar maximum state with smaller mean free path lengths to a nearly static solar minimum state having larger mean free path lengths for ACRs in the heliosphere. By mid-1994 the outer heliosphere, being closer to the ACR source, is very near a steady state in regard to the ACR intensities, while the inner heliosphere, remote from the ACR source, approaches this state more slowly. The steady state conditions in the outer heliosphere during the 1994 to 1999 period bring about rigidity-dependent radial intensity gradients that, along with the $e^r$ form for the ACR intensities as a function of helioradius, is predicted by simple convection/diffusion, the force field model [*Gleeson and Axford*, 1968], and both a spherically symmetric [*Hill*, 2001] and a more sophisticated [*Steenberg and Moraal*, 1996; *Steenberg*, 1998] numerical solution to the Fokker-Planck equation. As the Voyager spacecraft move through the distant heliosphere, the spatial ACR distribution is reflected in the time-intensity profiles because the innate temporal dependence is very small. This indicates that the large exponential growth of the low-rigidity ACR intensities is due primarily to the spacecraft motion through positive radial gradients, and not significantly to continued temporal variation of the ACR-related properties after 1994.

[36] The support for this interpretation is (1) the prevalence of the $1 - e^{-t/\tau}$ form for the higher-energy ACR and GCR recovery profiles [*McDonald et al.*, 2000b, 2002], coupled with (2) the ability this form has to fit our high-energy and 1-AU ACR O data. (3) This form, in combination with an exponential growth factor (equation (1)) is successful in fitting the lower-rigidity ACRs, with (4) a surprising similarity in the time constants $\tau$, suggesting a common mechanism (i.e., the rate of changing IP conditions) controlling the early recovery. (5) The distinct change

from the initial recovery form to sustained exponential growth along with the (6) rigidity-dependent nature of this exponential growth (in contrast to the similarity of the recoveries over a wide range of rigidities before mid-1994) strongly suggests that a second mechanism (i.e., spacecraft motion through rigidity-dependent positive intensity gradients) is at work during the late recovery. (7) Comparing the time-intensity profiles in this paper with the evolving energy spectra presented by *Hill et al.* [2002], we see that the initial recovery period also coincides with the period during which the energies of the peaks of the ACR spectra change rapidly with time, as would be expected from diffusion dominated transport and is shown by straightforward numerical modeling [*Hill*, 2001]. (8) After 1994 the energy of peak ACR intensity remains unchanged within observational limits, which agrees with a numerical transport model [*Hill*, 2001] that also accounts for the V1 and V2 motion. In this model the rate of the spectral peak shift decreases after equilibrium is established and spacecraft movement toward the ACR source becomes primarily responsible for the energy peak shift resulting from the "unfolding" of the spectrum. However, it should be noted that the observations exhibit a peak energy that changes less than the models, which would be consistent with an ACR source much more distant than is generally expected [*Hill et al.*, 2002], or otherwise remains to be fully understood. (9) As was shown by *Hill et al.* [2002], a comparison of 1996 ACR energy spectra in the inner and outer heliosphere is consistent with diffusion-dominated transport from the outer to the inner heliosphere, just as is described here. It would be difficult to explain, assuming temporal variations, why the outer heliospheric low-energy ACR intensities continued to increase at a faster rate than in the inner heliosphere, since, as with the high-energy ACRs, outer-to-inner heliospheric transport establishes the expectation that the outer heliospheric ACR intensities should approach an asymptote sooner than those in the inner heliosphere. We do point out that the apparently later onset of ACR recovery in the inner heliosphere complicates the simple diffusion-dominated transport interpretation. (10) A simple spherically symmetric, time, space, and energy dependent numerical solution to the cosmic ray transport equation [*Hill*, 2001] reproduces the late recovery data quantitatively using very few assumptions and with merely a cursory search of parameter space. That is, just by selecting the model parameters such that the numerical solution approximately reproduced a single ACR spectrum at one spacecraft at one time, the model is able not only to predict the rate of recoveries seen at the Voyager spacecraft but even generally agrees with the 1-AU data as well [*Hill*, 2001].

[37] **Acknowledgments.** Shadia Rifai Habbal thanks Conrad D. Steenberg for his assistance in evaluating this paper.

## References

Burlaga, L. F., F. B. McDonald, M. L. Goldstein, and A. J. Lazurus, Cosmic ray modulation and turbulent interaction regions near 11 AU, *J. Geophys. Res.*, *90*, 12,027–12,039, 1985.

Christian, E. R., et al., Observations of the solar modulation of galactic and anomalous cosmic rays during solar minimum, *Proc. 26th Int. Cosmic Ray Conf.*, *7*, 519–522, 1999.

Cummings, A. C., et al., Anomalous cosmic ray oxygen gradients throughout the heliosphere, *Geophys. Res. Lett.*, *22*, 341–344, 1995.

Cummings, A. C., E. C. Stone, B. Klecker, R. G. Marsden, R. A. Mewaldt, D. V. Reames, K. J. Trattner, T. T. von Rosenvinge, and W. R. Webber, Intensity gradients of anomalous cosmic ray oxygen throughout the heliosphere, *Proc. 25th Int. Cosmic Ray Conf.*, *2*, 257–260, 1997.

Cummings, A. C., E. C. Stone, and C. D. Steenberg, Composition of anomalous cosmic rays and other heliospheric ions, *Astrophys. J.*, *578*, 194–210, 2002.

Fisk, L. A., B. Kozlovsky, and R. Ramaty, An interpretation of the observed oxygen and nitrogen enhancements in low-energy cosmic rays, *Astrophys. J.*, *190*, L35–L37, 1974.

Garcia-Munoz, M., G. M. Mason, and J. A. Simpson, A new test for solar modulation theory: The 1972 May–July low-energy galactic cosmic ray proton and helium spectra, *Astrophys. J.*, *182*, L81–L84, 1973.

Gleeson, L. J., and W. I. Axford, Solar modulation of galactic cosmic rays, *Astrophys. J.*, *154*, 1011–1026, 1968.

Gloeckler, G., J. Geiss, H. Balsiger, L. A. Fisk, A. B. Galvin, F. M. Ipavich, K. W. Ogilvie, R. von Steiger, and B. Wilken, Detection of interstellar pick-up hydrogen in the solar system, *Science*, *261*, 70–73, 1993.

Hamilton, D. C., M. E. Hill, R. B. Decker, and S. M. Krimigis, Temporal and spatial variations in the spectra of low energy ions in the outer heliosphere, *Proc. 25th Int. Cosmic Ray Conf.*, *2*, 261–264, 1997.

Hamilton, D. C., M. E. Hill, G. Gloeckler, R. B. Decker, and S. M. Krimigis, Anomalous cosmic ray spectra in the outer heliosphere: 1992–1998, *Proc. 26th Int. Cosmic Ray Conf.*, *7*, 535–538, 1999.

Hill, M. E., Transport phenomena of anomalous cosmic rays during the recovery phase of solar cycle 22, Ph.D. thesis, Univ. of Maryland, College Park, Md., 2001.

Hill, M. E., D. C. Hamilton, and S. M. Krimigis, Periodicity of 151 days in outer heliospheric anomalous cosmic ray fluxes, *J. Geophys. Res.*, *106*, 8315–8322, 2001a.

Hill, M. E., D. C. Hamilton, J. E. Mazur, and S. M. Krimigis, The 1992–2000 recovery of anomalous cosmic ray oxygen throughout the heliosphere, *Proc. 27th Int. Cosmic Ray Conf.*, *10*, 4247–4250, 2001b.

Hill, M. E., D. C. Hamilton, and S. M. Krimigis, Evolution of anomalous cosmic-ray oxygen and helium energy spectra during the solar cycle 22 recovery phase in the outer heliosphere, *Astrophys. J.*, *572*, L169–L172, 2002.

Hovestadt, D., O. Vollmer, G. Gloeckler, and C. Y. Fan, Differential energy spectra of low-energy (<8.5 MeV per nucleon) heavy cosmic rays during solar quiet times, *Phys. Rev. Lett.*, *31*, 650–653, 1973.

Jokipii, J. R., The anomalous component of cosmic rays, in *Physics of the Outer Heliosphere*, edited by S. Grzedzielski and D. E. Page, pp. 169–178, Pergamon, New York, 1990.

Jokipii, J. R., and D. A. Kopriva, Effects of particle drift on the transport of cosmic rays, III, Numerical models of galactic cosmic-ray modulation, *Astrophys. J.*, *234*, 384–392, 1979.

Jokipii, J. R., E. H. Levy, and W. B. Hubbard, Effects of particle drift on cosmic-ray transport, I, General properties, application to solar modulation, *Astrophys. J.*, *213*, 861–868, 1977.

Krimigis, S. M., T. P. Armstrong, W. I. Axford, C. O. Bostrom, C. Y. Fan, G. Gloeckler, and L. J. Lanzerotti, The low energy charged particle (LECP) experiment on the Voyager spacecraft, *Space Sci. Rev.*, *21*, 329–354, 1977.

Krimigis, S. M., R. B. Decker, D. C. Hamilton, and M. E. Hill, Energetic ions in the outer heliosphere, 1992–1997, *Proc. 25th Int. Cosmic Ray Conf.*, *1*, 393–396, 1997.

Mason, G. M., D. C. Hamilton, P. H. Walpole, K. F. Heuerman, T. L. James, M. H. Lennard, and J. E. Mazur, LEICA: A low energy ion composition analyzer for the study of solar and magnetospheric heavy ions, *IEEE Trans. Geosci. Remote Sens.*, *31*, 549–556, 1993.

Mazur, J. E., G. M. Mason, J. B. Blake, B. Klecker, R. A. Leske, M. D. Looper, and R. A. Mewaldt, Anomalous cosmic ray argon and other rare elements at 1–4 MeV/nucleon trapped within the Earth's magnetosphere, *J. Geophys. Res.*, *105*, 21,015–21,023, 2000.

McDonald, F. B., B. J. Teegarden, J. H. Trainor, and W. R. Webber, The anomalous abundance of cosmic-ray nitrogen and oxygen nuclei at low energies, *Astrophys. J.*, *187*, L105–L108, 1974.

McDonald, F. B., A. Barnes, L. F. Burlaga, P. Gazis, J. Mihalov, and R. S. Selesnick, Effects of the intense solar activity of March/June 1991 observed in the outer heliosphere, *J. Geophys. Res.*, *99*, 14,705–14,715, 1994.

McDonald, F. B., A. Lukasiak, and W. R. Webber, Pioneer 10 and Voyager 1 observations of anomalous cosmic-ray hydrogen in the outer heliosphere, *Astrophys. J.*, *446*, L101–L104, 1995.

McDonald, F. B., N. Lal, and R. E. McGuire, Cosmic ray recovery and the solar minimum phase of solar cycle 22: An interim report, *J. Geophys. Res.*, *103*, 373–379, 1998.

McDonald, F. B., L. F. Burlaga, R. E. McGuire, and N. F. Ness, The onset of long-term cosmic ray modulation in cycle 23 coupled with a transient increase of anomalous cosmic rays in the distant heliosphere, *J. Geophys. Res.*, *105*, 20,997–21,003, 2000a.

McDonald, F. B., B. Heikkila, N. Lal, and E. C. Stone, The relative recovery of galactic and anomalous cosmic rays in the distant heliosphere: Evidence for modulation in the heliosheath, *J. Geophys. Res.*, *105*, 1–8, 2000b.

McDonald, F. B., B. Klecker, R. E. McGuire, and D. V. Reames, Relative recovery of galactic and anomalous cosmic rays at 1 AU: Further evidence for modulation in the heliosheath, *J. Geophys. Res.*, *107*(A8), 1156, doi:10.1029/2001JA000206, 2002.

Mewaldt, R. A., et al., The return of the anomalous cosmic rays to 1 AU in 1992, *Geophys. Res. Lett.*, *20*, 2263–2266, 1993.

Möbius, E., D. Hovestadt, B. Klecker, M. Scholer, G. Gloeckler, and F. M. Ipavich, Direct observation of $He^+$ pick-up ions of interstellar origin in the solar wind, *Nature*, *318*, 426–429, 1985.

Parker, E. N., The passage of energetic charged particles through interplanetary space, *Planet. Space Sci.*, *13*, 9–49, 1965.

Pesses, M. E., J. R. Jokipii, and D. Eichler, Cosmic ray drift, shock wave acceleration, and the anomalous component of cosmic rays, *Astrophys. J.*, *246*, L85–L88, 1981.

Reames, D. V., L. M. Barbier, and T. T. von Rosenvinge, WIND/EPACT observations of anomalous cosmic rays, *Adv. Space Res.*, *19*, 809–812, 1997.

Selesnick, R. S., A. C. Cummings, R. A. Leske, R. A. Mewaldt, E. C. Stone, and J. R. Cummings, Solar cycle dependence of the geomagnetically trapped anomalous cosmic rays, *Geophys. Res. Lett.*, *27*, 2349–2352, 2000.

Steenberg, C. D., Modelling of anomalous and galactic cosmic ray modulation in the outer heliosphere, Ph.D. thesis, Potchefstroom Univ. for Christian Higher Education, Potchefstroom, South Africa, 1998.

Steenberg, C. D., and H. Moraal, An acceleration/modulation model for anomalous cosmic ray hydrogen in the heliosphere, *Astrophys. J.*, *463*, 776–783, 1996.

Stone, E. C., A. C. Cummings, and W. R. Webber, The distance to the solar wind termination shock in 1993 and 1994 from observations of anomalous cosmic rays, *J. Geophys. Res.*, *101*, 11,017–11,025, 1996.

---

D. C. Hamilton and M. E. Hill, Department of Physics, University of Maryland, College Park, MD 20742-4111, USA. (douglas.c.hamilton@umail.umd.edu; mehill@umd.edu)

S. M. Krimigis, Applied Physics Laboratory, The Johns Hopkins University, 11100 Johns Hopkins Road, Laurel, MD 20723-6099, USA. (Tom.Krimigis@jhuapl.edu)

J. E. Mazur, Space Sciences Department, The Aerospace Corporation, M2/259, 2350 E. El Segundo Blvd, El Segundo, CA 90245-4691, USA. (Joseph.E.Mazur@aero.org)